Pairing Gap and In-Gap Excitations in Trapped Fermionic Superfluids

J. Kinnunen *et al.*

Science **305**, 1131 (2004);
DOI: 10.1126/science.1100782

Pairing Gap and In-Gap Excitations in Trapped Fermionic Superfluids

J. Kinnunen, M. Rodríguez, P. Törmä*

We consider trapped atomic Fermi gases with Feshbach-resonance enhanced interactions in pseudogap and superfluid temperatures. We calculate the spectrum of radio-frequency (or laser) excitations for transitions that transfer atoms out of the superfluid state. The spectrum displays the pairing gap and also the contribution of unpaired atoms, that is, in-gap excitations. The results support the conclusion that a superfluid, in which pairing is a many-body effect, was observed in recent experiments on radio-frequency spectroscopy of the pairing gap.

Fermionic superfluidity and superconductivity appear in several systems in nature, such as metals, cuprates, and helium. In the limit of weak interparticle interaction, the Bardeen-Cooper-Schrieffer (BCS) theory of superconductivity has been successful in explaining the observed phenomenon as a Bose-Einstein Condensation (BEC) of weakly bound momentum-space pairs. In the limit of strong interactions, spatially small, strongly bound pairs are formed and undergo BEC. The intriguing question about the nature of the crossover from BCS pairing to BEC of dimers was theoretically addressed in 1980 (*1*, *2*) and is closely related to uncovering the nature of high-temperature superconductivity. Trapped fermionic atoms offer a system in which the crossover can be scanned by tuning the interparticle scattering length using Feshbach resonances (*3*–*7*). At the crossover region, the scattering length diverges and a universal behavior, independent of any length scale, is expected. The system is also genuinely mesoscopic as a result of the trapping potential for the atoms. Here, we consider spectroscopic signatures of pairing in these systems at the onset of the superfluid transition and show that the mesoscopic nature of the system leads to pronounced signatures from unpaired atoms, which can also be understood as in-gap excitations. The results are in agreement with the experimental results in (*8*).

The single-particle excitation spectrum of a fermionic superfluid is expected to show an energy gap. A spectroscopic method for observing the excitation gap in atomic Fermi gases has been proposed (*9*–*11*). Radio-frequency (RF) spectroscopy has been used for observing mean fields (*12*, *13*) and, very recently, the excitation gap (*8*). Laser or RF fields are used for transferring atoms out of the superfluid state to a normal one. The superfluid state originates from the pairing of atoms in two different internal states, say $|1\rangle$ and $|2\rangle$. The field drives a transition from $|2\rangle$ to a third state, $|3\rangle$. Atoms in state $|3\rangle$ are not paired; that is, they are in the normal state. The idea is closely related to observing the superconductor–normal metal current in metals and, similarly, it reflects the density of states and displays the excitation gap. In this case, however, the superfluid-normal interface is realized by internal states of the atom, not by a spatial boundary. The response, in the case of atoms, is qualitatively different from that of metals because of the exact momentum conservation in atomic transitions driven by homogeneous fields. Here, we calculate the response of this process, that is, the spectrum as a function of the detuning of the RF field, taking into account the mesoscopic nature of the sample, that is, the trapping potential. This leads to pronounced signatures that can be used to confirm the onset of the excitation gap and the superfluid transition.

In the high critical temperature (T_c) region of the BEC-BCS crossover, the BCS theory, in its simplest form, is expected to be incapable of describing the effects of strong interactions, such as the formation of a pseudogap. In atomic Fermi gases, the vicinity of the Feshbach resonance is associated with strong interactions, and preformed pairs causing a pseudogap to exist even above the critical temperature. The excitation gap, therefore, has contributions both from the superfluid gap (Δ_{sf}) and the pseudogap (Δ_{pg}). The many-body state is affected also by the existence of the molecular bound state, which actually causes the Feshbach-resonance phenomenon. These issues are considered in recent work on resonance superfluidity theory (*14*–*17*). We use such an approach for calculating the equilibrium state of the system (*18*).

The interaction with the RF or laser field is introduced as a perturbation, and the response is calculated to the second order in the perturbation Hamiltonian. This corresponds to a Fermi golden rule type of derivation of the spectrum and allows a treatment of the complex many-body state with reasonable accuracy. The transfer Hamiltonian H_T, describing the effect of the field, couples states $|2\rangle$ and $|3\rangle$ (*18*). The offset from the resonance of the transition between $|2\rangle$ and $|3\rangle$ is given by the RF field detuning $\delta = E_{RF} - (E_3 - E_2)$, where E_{RF}, E_3, and E_2 are the energies of the RF photon and of the states $|3\rangle$ and $|2\rangle$, respectively. The spectrum is obtained from the response $I(\delta) = \langle \dot{N}_3 \rangle$, where N_3 is the number of atoms in state $|3\rangle$, by neglecting terms of higher than second order in H_T in the derivation (*18*). In the case of metals, such quantity would give the current $I(V)$, where V is voltage, over the superconductor–normal metal tunneling junction.

Trapped atomic gases have an inhomogeneous density distribution $n(\mathbf{r})$; therefore, a spatially varying superfluid order parameter is expected. We treat the problem in the local density approximation, that is, we solve the equilibrium state by including $n(\mathbf{r})$ given by the Thomas-Fermi distribution as a position-dependent parameter (*18*, *19*). Figure 1 presents the position dependence of the atom density and the superfluid gap. This shows that only the atoms in the middle of the trap are condensed. Figure 2 shows the fraction of condensed atoms and the mean (averaged over r) superfluid gap and pseudogap as functions of temperature. The parameters used in calculating the results in Figs. 1 to 3 correspond to the experiments in figure 3 of (*8*) and are given in (*18*).

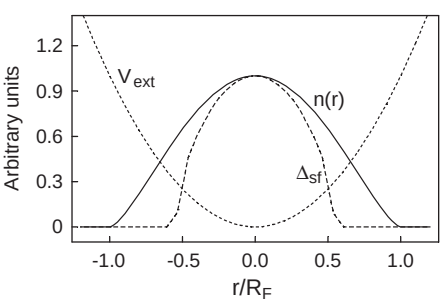

Fig. 1. The superfluid Δsf gap and the atom density n(r) as functions of position at temperature $T = 0.2\ T_F$, where T_F is the Fermi temperature. Resonance-superfluidity theory incorporating a pseudogap, together with Thomas-Fermi distribution in the local density approximation, is used. Only the atoms in the middle of the trap are condensed, whereas the atoms closer to the borders are either free or in the pseudogap regime. The critical temperature in the middle of the trap is $T_c \approx 0.3\ T_F$. V_{ext} is the external potential as a function of distance in units of Thomas-Fermi radius, r/R_F.

Department of Physics, NanoScience Center, Post Office Box 35, FIN-40014, University of Jyväskylä, Finland.

*To whom correspondence should be addressed. E-mail: paivi.torma@phys.jyu.fi

The spectra $I(\delta)$ at different temperatures are plotted in Fig. 3. The peak at the zero detuning, $\delta = 0$, originates from free (unpaired) atoms. Another peak, shifted right from the zero, appears with decreasing temperature. The shift reflects the excitation gap, that is, the energy needed for breaking a pair. The free-atom peak gradually vanishes when the temperature is lowered and the atoms at the borders of the trap become paired. The disappearance of the free-atom peak shows that the border atoms have reached the pseudogap regime (*18*) and that the atoms in the middle of the trap are well below the superfluid transition temperature (*20*). We have neglected the effect of the mean (Hartree-Fock) field energy shifts (*18*) because they appear absent in the experiments (*8*, *13*).

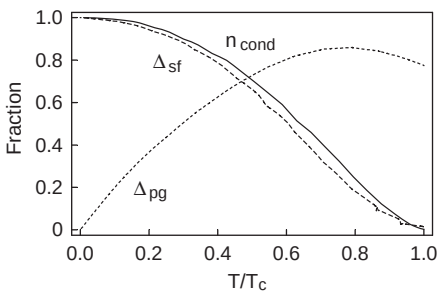

Fig. 2. The mean superfluid gap (Δ_{sf}) and pseudogap (Δ_{pg}) as functions of temperature. The fraction of condensed atoms n_{cond} is defined as the fraction of atoms for which the temperature is below the local critical temperature. The temperature $T \approx 0.7\ T_c$ corresponds to $T = 0.2\ T_F$, showing that the superfluid gap distribution in Fig. 1 corresponds to a condensate fraction of $n_{cond} \approx 0.3$.

In a corresponding spatially homogeneous system, instead of the free-atom peak at zero detuning, a quasiparticle peak, shifted left from the zero, appears at high temperatures (*11*). The shift is to the left, in the opposite direction of that of the pair peak, because thermal quasiparticles of the superfluid already possess the excess gap energy, that is, energy is gained in the RF transfer process (*21*). As Fig. 3 shows, such quasiparticle peaks appearing in a homogeneous system are now shadowed by trapping effects and by the free-atom peak. The unpaired atoms in Fig. 3 can, however, be understood as in-gap excitations or quasiparticles. Instead of the local density approximation, inhomogeneous superfluids can be described by the Bogoliubov–de Gennes equations. Solving the equations in a trap geometry (*10*, *22*) results in in-gap excitations whose energies lie below the maximum (at the point of highest density) gap energy. The wave functions of these excitations are located at the edges of the trap; they correspond to the free atoms at the borders of the trap in the local-density treatment. The free atoms in Fig. 3 and observed in (*8*) can thus be understood as in-gap excitations of an inhomogeneous superfluid.

The spectra in Fig. 3 are in excellent qualitative agreement with the experimental results in (*8*). They also agree well quantitatively with figure 3 of (*8*). The shift of the pair peak, which gives the excitation gap, is at temperatures $T' \leq 0.2\ T_F$, about $0.2\ E_F$ in (*8*) and $0.3\ E_F$ for $T \leq 0.1\ T_F$, according to our calculation. The widths of the peaks, which are determined by the gap, are about $0.3\ E_F$ and $0.4\ E_F$, respectively. The critical temperature at the center of the trap is in our case $T_c \sim 0.3\ T_F$, which may be used to estimate that in (*8*) it is ~0.2 to $0.25\ T_F$. The temperatures T' in the experiment are determined in the BEC limit as a result of the lack of precise thermometry in the unitarity limit. The adiabatic passage to the unitarity limit, where the spectra are actually measured, is expected to reduce the temperature as a result of entropy conservation so that $T < T'$ (*23*). This is consistent with the observation that the pair peak in Fig. 3 starts to appear at $T \sim 0.35\ T_F$ and is clearly visible at $T \sim 0.2\ T_F$, but in (*8*) it appears and is clearly visible already at higher (BEC limit) temperatures of $T' \sim 0.75\ T_F$ and $T' \sim 0.45\ T_F$, respectively. The sensitivity of the free-atom (quasiparticle) peak to temperature and the possibility of direct comparison between theory and experiment may offer a route for developing a precise thermometry for the crossover region.

We emphasize that those spectra in (*8*) where the free-atom peak has disappeared correspond to Fig. 3, H to J, where more than 80% of the atoms are condensed. This indicates that the pairing observed at the lowest temperatures in (*8*) corresponds to a superfluid. At higher temperatures, either a pseudogap or a combined effect of a superfluid gap and a pseudogap occurs. In summary, the results presented here support the conclusion that a superfluid, in which pairing is a many-body effect, was observed in (*8*). The mesoscopic nature of these novel Fermi superfluids shows up in an intriguing way.

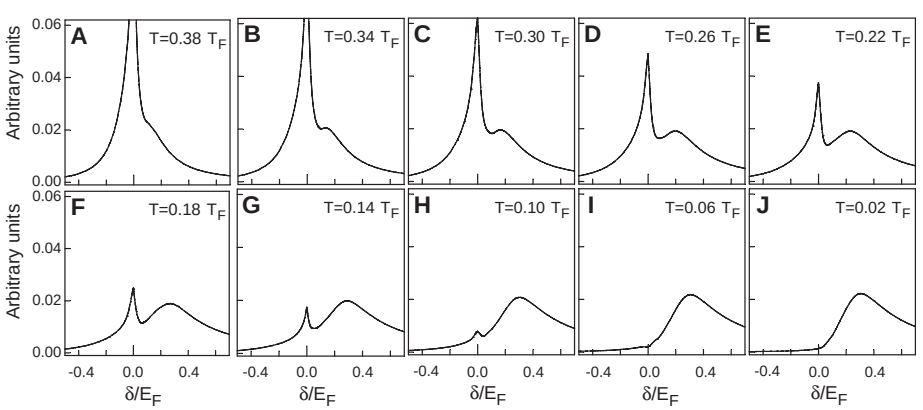

Fig. 3. The spectra of the considered RF transition as a function of the RF field detuning δ for several temperatures. The peak at $\delta = 0$ is caused by free atoms. A peak shifted to the right from the zero gradually appears for lower temperatures, corresponding to paired atoms; the shift of the peak from the zero detuning gives the energy gap in the single-particle excitation spectrum. The shift, that is, the gap, grows with decreasing temperature. The plots also show the disappearance of the free-atom peak when the atoms at the borders of the trap enter the pseudogap regime and become paired. The critical temperature in the middle of the trap is $T_c \approx 0.3\ T_F$. At the temperature $T = 0.1\ T_F$, more than 80% of the atoms are condensed. The parameters used in the calculation correspond to the experiments in Fig. 3 of (*8*). The gas is in the unitarity limit, that is, close to the Feshbach resonance, which is the expected high-T_c regime for the system. E_F, Fermi energy.

References and Notes

1. A. J. Leggett, *Modern Trends in the Theory of Condensed Matter* (Springer-Verlag, Berlin, 1980), p. 13.
2. P. Nozières, S. Schmitt-Rink, *J. Low Temp. Phys.* **59**, 195 (1985).
3. C. A. Regal, M. Greiner, D. S. Jin, *Phys. Rev. Lett.* **92**, 040403 (2004).
4. M. Bartenstein *et al.*, *Phys. Rev. Lett.* **92**, 120401 (2004).
5. M. W. Zwierlein *et al.*, *Phys. Rev. Lett.* **92**, 120403 (2004).
6. J. Kinast, S. L. Hemmer, M. E. Gehm, A. Turlapov, J. E. Thomas, *Phys. Rev. Lett.* **92**, 150402 (2004).
7. M. Bartenstein *et al.*, *Phys. Rev. Lett.* **92**, 203201 (2004).
8. C. Chin *et al.*, *Science* **305**, 1128; published online 22 July 2004 (10.1126/science.1100818).
9. P. Törmä, P. Zoller, *Phys. Rev. Lett.* **85**, 487 (2000).
10. G. M. Bruun, P. Törmä, M. Rodríguez, P. Zoller, *Phys. Rev. A.* **64**, 033609 (2001).
11. J. Kinnunen, M. Rodríguez, P. Törmä, *Phys. Rev. Lett.* **92**, 230403 (2004).
12. C. A. Regal, D. S. Jin, *Phys. Rev. Lett.* **90**, 230404 (2003).
13. S. Gupta *et al.*, *Science* **300**, 1723 (2003).
14. M. Holland, S. J. J. M. F. Kokkelmans, M. L. Chiofalo, R. Walser, *Phys. Rev. Lett.* **87**, 120406 (2001).
15. E. Timmermans, K. Furuya, P. W. Milonni, A. K. Kerman, *Phys. Lett. A* **285**, 228 (2001).
16. Y. Ohashi, A. Griffin, *Phys. Rev. Lett.* **89**, 130402 (2002).
17. J. Stajic *et al.*, *Phys. Rev. A.* **69**, 063610 (2004).
18. Materials and methods are available as supporting material on *Science* Online.

19. M. L. Chiofalo, S. J. J. M. F. Kokkelmans, J. N. Milstein, M. J. Holland, *Phys. Rev. Lett.* **88**, 090402 (2002).
20. The pronounced free-atom peak at the zero detuning clearly reflects the strong dependence of the order parameter on density and the trapping potential. In the case of a very smooth density dependence of the energy gap, one would expect simply a broadening of the pair peak. Such a behavior was actually observed in the experiments probing mean fields (*12*, *13*). There, only one peak was observed and the effect of the trapping potential was a considerable broadening of the peak.
21. Note that because not only energy but also momentum is exactly conserved in the transfer process, these particles cannot be transferred at zero detuning. This is in contrast to superconductor–normal metal junctions where thermal quasiparticle currents flow freely for below-gap voltages.
22. M. A. Baranov, *JETP Lett.* **70**, 396 (1999).
23. The precise relation between T' and T at the unitarity limit is not known, but the analysis in the case of a noninteracting Fermi gas (*24*) supports this argument.
24. L. D. Carr, G. V. Shlyapnikov, Y. Castin, *Phys. Rev. Lett.* **92**, 150404 (2004).
25. We thank C. Chin and R. Grimm for a stimulating exchange of results and very useful discussions. We acknowledge financial support from the Academy of Finland (Project Nos. 53903 and 205470) and the Emil Aaltonen Foundation.

Supporting Online Material
www.sciencemag.org/cgi/content/full/1100782/DC1
Materials and Methods
References and Notes

26 May 2004; accepted 13 July 2004
Published online 22 July 2004;
10.1126/science.1100782
Include this information when citing this paper.

Sudden Onset of Pitting Corrosion on Stainless Steel as a Critical Phenomenon

C. Punckt,[1] M. Bölscher,[1] H. H. Rotermund,[1] A. S. Mikhailov,[1] L. Organ,[2] N. Budiansky,[3] J. R. Scully,[3] J. L. Hudson[2]*

Stainless steels undergo a sharp rise in pitting corrosion rate as the potential, solution concentration, or temperature is changed only slightly. We report experiments using real-time microscopic in situ visualizations that resolve the nucleation and evolution of individual pits during the transition. They suggest that the sudden onset of corrosion is explained by an explosive autocatalytic growth in the number of metastable pits and that stabilization of individual pits takes place only later. This finding agrees with a theoretical approach treating the onset of pitting corrosion as a cooperative critical phenomenon resulting from interactions among metastable pits, and it extends perspectives on the control and prevention of corrosion onset.

All commonly used stainless steels and other passive-film–forming metals, which are designed to be corrosion-resistant, can nevertheless undergo localized pitting corrosion, which rapidly leads to their failure. The total annual costs due to corrosion in the United States are estimated at 3% of the gross national product (*1*), and a third of chemical plant failures are attributed to localized corrosion (*2*). Localized corrosion is preceded by the appearance of metastable pits: tiny corrosion seeds the size of a few micrometers developing on the metal surface, which is naturally protected by an oxide layer. Each pit produces a small spike of a few seconds duration in the electrical current, indicating an anodic reaction, and the spike then dies out. Experimental and theoretical studies have largely clarified the mechanism for the initiation of these microscopic pits as being caused by localized electrodissolution of metal at surface defects and inclusions (*3*–*8*).

[1]Abteilung Physikalische Chemie, Fritz-Haber-Institut der Max-Planck-Gesellschaft, Faradayweg 4-6, 14195 Berlin, Germany. [2]Department of Chemical Engineering, [3]Department of Material Science and Engineering, 102 Engineers' Way, University of Virginia, Charlottesville, VA 22904–4741, USA.

*To whom correspondence should be addressed. E-mail: hudson@virginia.edu

Pitting corrosion shows a sharp rise in corrosion rate that occurs with only a small change in conditions, such as applied potential, corrodant concentrations, or temperature (*9*). This corresponds to a sudden transition from a low-activity regime with a few metastable pits to a state with high pitting activity (*10*, *11*). The transition has been explained by a stabilization of individual pits (*12*). As an alternate explanation, we suggest that the onset of pitting corrosion represents a cooperative critical phenomenon. In previous investigations, temporal statistical correlations between the spikes in the total current have been found (*13*, *14*), indicating some memory in the pitting process (*15*). A stochastic spatiotemporal model of the corrosion onset has been proposed (*16*). According to this model, electrochemical reactions at a metastable pit change ion concentrations and weaken the protective film over defect sites. Each pit enhances the probability of appearance of further pits at defect sites within a wide zone of weakened film around it. We show below that autocatalytic reproduction of pits can take place. Sudden transitions are thus associated with an explosive growth in the number of active pits. Stabilization of individual pits would occur only after the transition.

To distinguish between different approaches, microscopic in situ visualizations of the onset of pitting corrosion are needed. Several experimental methods have been used to investigate pitting corrosion on stainless steels. Distributions and characteristics of pitting sites on metal surfaces have been determined through microscopic inspection after the termination of corrosion (*5*, *17*, *18*). Changes in the thickness of the oxide layer in the vicinity of an active pit and the topography of surfaces before and after pitting events have been measured via scanning techniques in which spatial or temporal resolution is restricted (*19*, *20*). Optical microscopy was applied in situ to observe relatively large, already stable pits (diameter >10 μm) (*21*), and individual metastable pits were visualized by using pH-sensitive agar gels (*22*, *23*) that indicated interactions among active pits.

We present detailed, time-resolved, in situ visualizations of the onset of pitting corrosion directly in the electrolyte, using two different techniques: ellipsomicroscopy for surface imaging (EMSI) and specially adapted high-resolution contrast-enhanced optical microscopy. Both techniques are accompanied by parallel monitoring of the current. Thus, the temporal and spatial development of metastable pits is followed during the transition to pitting corrosion, and we can also differentiate between active and inactive pits.

Ellipsometry, based on the detection of the polarization rotation of the light reflected from the surface, has been used in an electrochemical cell to measure average thicknesses of oxide layers on metal surfaces (*24*, *25*). In contrast to intrinsically slow scanning ellipsometry methods, EMSI permits real-time observation of ultrathin layers on the entire surface area (*26*). Figure 1A displays four snapshots from an EMSI video sequence at an early corrosion stage, with space/time diagrams along two line segments, and the electrical current (movie S1A). Bright areas extending up to 100 μm are observed, with the intensity gradually fading toward the periphery. We interpret the observed brightness as revealing changes in the thickness of the protective oxide layer on the surface around an active pit. Changes in solution concentration around a pit can be ruled out as a source